Macromolecules **2004,** *37,* 709−715

4-Hexylbithieno[3,2-*b*:2′3′-*e*]pyridine: An Efficient Electron-Accepting Unit in Fluorene and Indenofluorene Copolymers for Light-Emitting Devices

Prashant Sonar, Jingying Zhang,[†] Andrew C. Grimsdale, and Klaus Müllen*

Max-Planck-Institut für Polymerforschung, Ackermannweg 10, D-55128 Mainz, Germany

Mathieu Surin, Roberto Lazzaroni, and Philippe Leclère

Service de Chimie des Matériaux Nouveaux, Centre de Recherche en Electronique et Photonique Moléculaires, Université de Mons-Hainaut, Place du Parc 20, B-7000 Mons, Belgium

Steve Tierney, Martin Heeney, and Iain McCulloch*

Merck Chemicals, Chilworth Science Park, University Parkway,
Southampton SO16 7QD, United Kingdom

Received September 8, 2003; Revised Manuscript Received December 5, 2003

ABSTRACT: 4-Hexylbithienopyridine has been prepared as a novel electron-accepting monomer for conjugated polymers. To test its electronic properties, alternating copolymers with fluorene and indenofluorene polymers have been prepared. The copolymers displayed reduction potentials about 0.5 V lower than for the corresponding fluorene and indenofluorene homopolymers, indicating much improved electron-accepting properties. Analysis of the microscopic morphology of thin films of the copolymers by AFM shows that they lack the extensive supramolecular order seen with the homopolymers, which is attributed to the bithienopyridine units disrupting the π-stacking. LEDs using these polymers as the emitting layer produce blue-green emission with low turn-on voltages with aluminum electrodes confirming their improved electron affinity. The indenofluorene copolymer displayed an irreversible red shift in emission at high voltages, which is attributed to oxidation of the indenofluorene units. This red shift occurred at higher potentials than for indenofluorene homopolymers in LEDs, suggesting that the heterocyclic moieties offer some protection against electrically promoted oxidation.

Introduction

Conjugated polymers have been the subject of considerable academic and industrial research in recent years due to their possible applications in optoelectronic devices such as field-effect transistors,[1] solar cells,[2] and light-emitting diodes (LEDs).[3,4] One major problem with organic polymers for such applications is that they are usually much better at accepting and transporting holes than electrons. This is a limiting factor in the development of LEDs as obtaining balanced charge injection and transport is necessary for obtaining high device efficiencies. One approach to improving electron injection and transport in conjugated polymers is to incorporate moieties with high electron affinities. For example, it has been shown that the electron-accepting properties of conjugated polymers can be improved by the introduction of pyridine units,[5] but unsubstituted pyridine units tend to reduce the solubility of the copolymers and attaching solubilizing groups onto pyridine is difficult. Accordingly, we were interested in exploring the potential of 4-alkylbithieno[3,2-*b*:2′,3′-*e*]pyridines as electron-accepting moieties for electronic materials. These monomers were anticipated to have high electron affinities due to the presence of the three electronegative heteroatoms, and soluble alkyl-substituted derivatives are readily accessible by condensation of aldehydes with 3-aminothiophene.[6,7] It was anticipated that halogenation would occur readily at the two thiophene α-positions (positions 2 and 6) to provide suitable comonomers for organometallic polycoupling reactions. Also, though this system is fully aromatic, there exists no uncharged Kekulé form in which substituents at the 2- and 6-positions are conjugated to each other, so that we were interested to see what effect this would have on the through conjugation.

Fluorene and indenofluorene were chosen as suitable comonomers to test the efficiency of the electron-accepting properties of our new monomer. Polyfluorenes[8] and polyindenofluorenes[9] have attracted considerable research interest in recent years as potential blue-emitting materials for LEDs. Both these classes of polymer have high LUMO energy levels and so are poor electron acceptors, so that low work-function metals such as calcium must be used as cathodes to obtain efficient emission. Since such metals are highly sensitive to air and water, this means that efficient encapsulation of the devices is required to prevent degradation of the electrodes. Accordingly, lowering the LUMO by improving the electron-accepting properties of the polymers and so enabling more air-stable metals to be used is highly desirable.

Another problem with fluorene and indenofluorene homopolymers is that of color instability due to the appearance of red-shifted emission bands. The red-shifted emission from these materials was initially attributed to the formation of excimers due to aggregation of the chains through $\pi-\pi$ stacking,[8,10] but more

---

[†] Current address: Key Laboratory for Supramolecular Structure and Materials of Ministry of Education, 119 Jiefang Road, Changchun 130023, P. R. China.

* Corresponding authors. E-mail: iain.mcculloch@mercknbsc.co.uk; muellen@mpip-mainz.mpg.de.

10.1021/ma035329u CCC: $27.50

recently it has been shown that the long wavelength emission from polyfluorenes arises from ketone defect sites produced by partial oxidation of the polymer chains.[11] We have shown that the appearance of this emission is suppressed by the attachment of aryl substituents to the methine bridges in polyfluorenes[12−14] and polyindenofluorenes.[15] This suppression is attributed to a combination of increased resistance to oxidation and to the bulky aryl substituents hindering exciton migration to defect sites by reducing interchain interactions. The red-shifted emission in polyfluorenes has also been reduced by blending them with hole-transporting materials,[16] which act as charge traps hindering exciton formation at the defect sites. The incorporation of an electron-accepting unit, particularly one which interferes with $\pi-\pi$ stacking, might therefore be expected to also suppress red-shifted emission, either by reducing the susceptibility of the methine bridges to oxidation by inductive reduction of the electron density there, by suppression of exciton formation at defect sites, or by hindering exciton migration.

We now report the synthesis of a novel 2,6-dibromobithienopyridine electron-accepting monomer and its alternating copolymers with fluorene and indenofluorene. We also report studies of their morphological, optical, and electrochemical properties to determine the effects of the new monomer on the copolymer.

Experimental Section

^{1}H and ^{13}C NMR spectra were recorded on a Bruker 250 or 400 MHz spectrometer using tetramethylsilane as an internal standard. Infrared spectra were measured as oils or as KBr pellets using a Perkin-Elmer spectrometer. Gel permeation chromatography (GPC) analysis against polystyrene standards was performed in THF on a Waters high-pressure GPC assembly with an M590 pump, μ-Styragel columns of 10^5, 10^4, 10^3, 500, and 100 Å, and a refractive index detector. UV−vis absorption spectra were obtained on a Perkin-Elmer Lambda 15 spectrophotometer. Photoluminescence spectra were recorded on a SPEX Fluorolog 2 type F212 steady-state fluorometer, using a 450 W xenon arc lamp as excitation source and a PMT R 508 photomultiplier as detector system. Thermal gravimetric analysis and differential scanning calorimetry (DSC) measurements were carried out on a Mettler 500 thermogravimetric analyzer and Mettler DSC 30, respectively. CV was performed on an EG&G Princeton Applied Research potentiostat, model 270, on 2 μm thick films deposited by solution-coating onto precleaned ITO as a working electrode with an area of 0.2 cm^2. After coating, the films were dried in a vacuum oven for 10 min. The measurements were carried out in acetonitrile solutions containing 0.1 M tetrabutylammonium fluorate (TBAF) as the supporting electrolyte, using Ag/AgCl as reference electrode and a platinum wire as counter electrode, and an internal ferrocene/ferrocenium (FOC) standard.

For AFM measurements, thin deposits were made by solvent casting on freshly cleaved muscovite mica substrates from dilute solutions (0.05 mg/mL); the solvent (THF) was evaporated slowly at room temperature in a solvent-saturated atmosphere. Tapping-mode atomic force microscopy was performed with a Nanoscope IIIa microscope from Digital Instruments operating at 25 °C; microfabricated silicon cantilevers with a spring constant of ~30 N/m were used.

LEDs were constructed on glass substrates coated with a transparent ITO electrode (ca. 10 Ω/cm^2), which were cleaned by successive ultrasonic treatments in acetone and isopropyl alcohol and dried under nitrogen. After treatment of the substrate with ozone at room temperature for 10 min, a hole injecting layer of poly(3,4-ethylenedioxythiophene):poly(styrenesulfonate) (PEDOT:PSS, Bayer Corp.) was deposited by spin-coating from an aqueous solution (1.3 wt %) at a spin rate of 1200 rpm onto the ITO substrates and cured at 100 °C for 30 min under vacuum. The emissive layers were prepared by spin-casting from chloroform solutions (10 mg/mL) and dried under vacuum overnight. A metal cathode of Al (~120 nm) was thermally evaporated in a vacuum evaporator (5×10^{-6} mbar) onto the polymer film through a mask; the area of each pixel was ca. 7 mm^2. The fabricated devices were sealed with cover glass/UV curing agent in a drybox under a nitrogen atmosphere. Device characteristics were measured using a Keithley 236 current/voltage source and Newport 818-SL optical power meter.

2,6-Dibromo-4-hexylbithieno[3,2-*b*:2′3′-*e*]pyridine: Monomer M1. A solution of heptanal (0.59 g, 5.16 mmol) and trifluoroacetic acid (0.10 g) in anhydrous DCM (50 mL) was added dropwise to a solution of 3-aminothiophene[6] (0.93 g, 9.38 mmol) in anhydrous DCM (50 mL) at −5 °C. The reaction mixture was stirred at room temperature for 1.5 h. Trifluoroacetic acid (1.07 g, 9.38 mmol) was added, and the reaction mixture was heated at reflux for 6 h. The solution was cooled to room temperature, and diethyl ether (150 mL) and water (30 mL) were added. The aqueous layer was basified with 0.5 N aqueous sodium hydroxide solution, and the organic layer was separated. The aqueous layer was extracted into diethyl ether (150 mL). The combined organic extracts were dried over sodium sulfate and concentrated in vacuo. Column chromatography eluting with DCM afforded 4-hexylbithieno-[3,2-*b*:2′3′-*e*]pyridine (0.58 g, 45%) as a red oil: Found: C 64.60, H 6.40, N 5.00, S 23.00%. Calculated for $C_{15}H_{17}NS_2$: C 65.40, H 6.23, N 5.09, S 23.28%. ^{1}H NMR (CDCl$_3$, 250 MHz): δ 7.75 (d, J = 6 Hz, 2H, Ar*H-2*,), 7.59 (d, J = 6 Hz, 2H, Ar*H-3*,), 3.16 (t, J = 7.5 Hz, 2H, ArC*H*$_2$,), 1.90 (m, 2H), 1.27−1.49 (m, 6H), 0.89 (t, J = 7.5 Hz, 3H). ^{13}C NMR (CDCl$_3$, 63 MHz): δ 156.2, 140.4, 130.7 (ArH-2), 129.7, 125.7 (ArH-3), 34.8, 31.9, 29.8, 28.3, 22.9, 14.4. MS (*m*/*z*): 275 (M$^+$).

A 2.5 M solution of butyllithium in hexanes (7.0 mL, 17.50 mmol) was added to a solution of 4-hexylbithieno[3,2-*b*:2′3′-*e*]-pyridine (2.00 g, 7.26 mmol) in anhydrous THF (30 mL) at −78 °C. The solution was stirred at −78 °C for 1 h and then at 0 °C for 5 h. The solution was cooled back down to −78 °C, and a solution of trimethyltin chloride (2.89 g, 14.52 mmol) in anhydrous THF (20 mL) was added dropwise. The reaction was stirred overnight (22 h) and allowed to attain room temperature. The reaction mixture was poured onto ice (50 mL) and extracted into diethyl ether (2 × 100 mL). The combined extracts were washed with 3% aqueous ammonia solution (100 mL) and water (100 mL), then dried over sodium sulfate, and concentrated in vacuo to yield a dark red oil. Kugelrohr distillation was used to remove some impurities from the bis(trimethyltin) intermediate; however, the pure material was not isolated. *N*-Bromosuccinimide (1.54 g, 8.65 mmol) was added to a solution of the crude bis(trimethyltin) intermediate (2.60 g, 4.33 mmol) in chloroform (20 mL). The reaction mixture was stirred at room temperature for 1.5 h. The reaction mixture was poured into water (25 mL) and extracted into diethyl ether (2 × 100 mL). The combined extracts were dried over sodium sulfate and concentrated in vacuo to yield a pale orange solid. Recrystallization twice from diethyl ether yielded 2,6-dibromo-4-hexylbithieno[3,2-*b*:2′3′-*e*]-pyridine (0.82 g, 1.89 mmol, 26%) as fine white needles; mp 123−125 °C. Found: C 41.56, H 3.41, N 3.19, S 14.02%. Calculated for $C_{15}H_{15}Br_2NS_2$: C 41.59, H 3.49, N 3.23, S 14.80%. ^{1}H NMR (CDCl$_3$, 400 MHz): δ 7.56 (s, 2H, Ar*H-3*), 2.96 (t, J = 7.5 Hz, 2H, ArC*H*$_2$,), 1.82 (m, 2H), 1.25−1.45 (m, 6H), 0.90 (t, J = 7.5 Hz, 3H). ^{13}C NMR (CDCl$_3$, 100 MHz): δ 154.8, 138.0, 131.2, 127.8 (ArH-3), 120.8, 34.3, 31.4, 29.3, 27.1, 22.4, 14.0. MS (*m*/*z*): 433 (M$^+$).

Polymer P1. To a stirred solution of 2,7 dibromo-9,9-dioctylfluorene (5.0 g, 9.1 mmol) in THF (70 mL) at −78 °C was added dropwise *n*-butyllithium in hexanes (7.6 mL, 2.5 M, 19 mmol) at −78 °C. The mixture was warmed to 0 °C for 15 min and then cooled back to −78 °C. 2-Isopropoxy-4,4,5,5-tetramethyl-1,3,2-dioxaborolane (4.0 g, 21.5 mmol) was added rapidly to the solution, and the resulting mixture was warmed to room temperature and stirred for 24 h. The mixture was then poured into water and extracted with diethyl ether. The

Scheme 1. Synthesis of Monomer M1

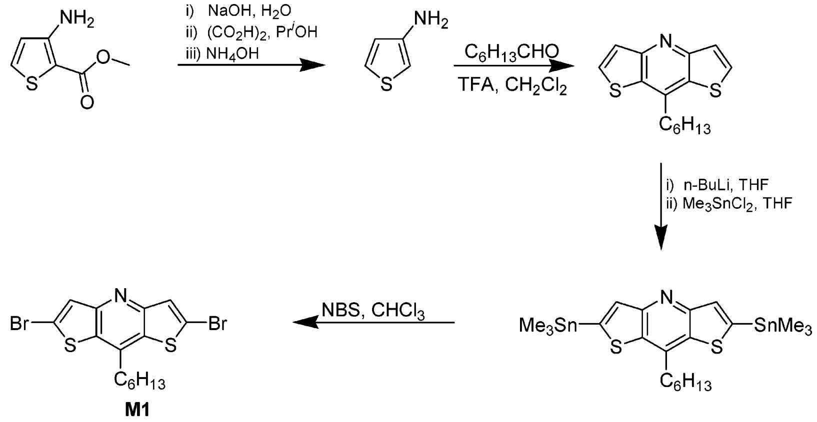

organic extract was washed with brine and dried over magnesium sulfate. The solvent was removed under reduced pressure, and the crude product was purified by column chromatography eluting with 2% ethyl acetate/hexane to give 2,7-bis(4,4,5,5-tetramethyl-1,3,2-dioxaborolan-2-yl)-9,9-dioctylfluorene (**M2**) as a pale yellow solid (3.80 g, 65%). HRMS: Calcd for $C_{41}H_{64}B_2O_4$: 642.59. Found: 642.37. ^{1}H NMR (250 MHz CD_2Cl_3): δ 7.83 (d, 2H), 7.76 (s, 2H), 7.73 (d, 2H), 2.05 (m, 4H), 1.44 (s, 24H), 1.25−1.09 (m, 20 H), 0.82 (t, 6H), 0.59 (m, 4H). ^{13}C NMR (62.5 MHz, CD_2Cl_3): δ 150.35, 143.82, 133.84, 128.74, 119.23, 83.51, 54.96, 39.36, 31.68, 29.89, 29.08, 29.00, 24.87, 23.50, 22.49, 13.96.

A solution of **M1** (0.300 g,0.466 mmol), **M2** (0.202 g,0.466 mmol), and $Pd(PPh_3)_4$ (0.020 g, 0.5 mol %) in a mixture of toluene (15 mL) and aqueous 2 M K_2CO_3 (10 mL) was refluxed with vigorous stirring for 72 h under N_2. The cooled mixture was poured into methanol (150 mL), and the precipitate was recovered by filtration and washed with dilute HCl. The precipitate was then extracted with acetone in a Soxhlet apparatus for 24 h. The dried residue was dissolved in dichloromethane and stirred with EDTA solution overnight. The residue of crude polymer was twice dissolved in chloroform and reprecipitated from methanol to give the copolymer **P1** as a yellow solid (0.2 g, 67%). Elemental analysis: Found: C 79.09, H 3.15, N 2.11, S 5.23%. Calculated: C 79.58; H 8.65, N 2.11, S 9.66%. GPC: M_n = 10 577 g/mol, M_w = 31 297 g/mol, D = 2.95. ^{1}H NMR (250 MHz, CD_2Cl_2): δ 7.88 (s, 2H), 7.82 (m, 2H), 7.59 (m, 2H), 7.24 (d, 2H) 3.10 (t, 2H) 2.1 (m, 6H), 0.9 (m, 40 H). ^{13}C NMR (62.5 MHz, CD_2Cl_2): δ 155.54, 152.60, 142.00, 141.86, 138.89, 128.40, 121.17, 120.99, 120.67, 40.58, 34.64, 32.13, 31.93, 30.29, 29.54, 25.11, 22.95, 14.18.

Polymer P2. *n*-Butyllithium in hexane (2.78 mL, 2.5 M, 3.65 mmol) was added to a solution of 2,8-dibromo-6,6′,12,12-tetraalkylindenofluorene (1.50 g, 1.7 mmol) in dry THF (30 mL) at −78 °C. The mixture was warmed to 0 °C for 15 min and then again cooled to −78 °C for 15 min. 2-Isopropoxy-4,4,5,5-tetramethyl-1,3,2-dioxaborolane (0.88 mL, 3.65 mmol) was added rapidly to the solution, and the resulting mixture was warmed to room temperature and stirred for 24 h. The mixture was poured into water and extracted with ether. The organic extracts were washed with brine and dried over magnesium sulfate. The solvent was removed by rotary evaporation, and the residue was purified by column chromatography on silica (eluting with 10% ethyl acetate in hexane) to give 2,8-bis(4,4,5,5-tetramethyl-1,3,2-dioxaborolan-2-yl)-6,6′,12,12-tetraalkylindenofluorene (**M3**) as a white solid (1.2 g, 74%). Found: C 80.47, H 10.49%; *M* 954.97. Calculated for $C_{64}H_{100}B_2O_4$: C 80.48, H 10.55%; *M* 955.13. ^{1}H NMR (250 MHz, $CDCl_3$): δ 7.72−7.78 (d, 4H), 7.70 (s, 4H), 2.02 (m, 8H), 1.38 (s, 24H), 1.25−1.09 (m, 40H), 0.81 (t, 12H), 0.59 (m, 8H). ^{13}C NMR (62.5 MHz, $CDCl_3$): δ 151.05, 150.75, 144.81, 141.32, 133.85, 129.09, 119.09, 114.80, 84.06, 40.89, 32.16, 30.34, 29.62, 25.25, 24.25, 22.95, 14.19.

A solution of **M1** (88 mg, 0.209 mmol) and **M3** (0.2 g, 0.209 mmol) and $Pd(PPh_3)_4$ (0.020 g, 0.5 mol %) in a mixture of toluene (6 mL) and aqueous 2 M K_2CO_3 (4 mL) was refluxed with vigorous stirring for 72 h under N_2. The cooled mixture was then poured into methanol (150 mL). The precipitate was recovered by filtration and washed with dilute HCl and then extracted with acetone for 24 h in a Soxhlet apparatus. The polymer was then dissolved in dichloromethane, and the solution was stirred with EDTA solution overnight and then dried. The residue was then twice dissolved in chloroform and reprecipitated from methanol to give **P2** as a yellow solid (0.15 g, 75%). Elemental Analysis: Found: C 73.16, H 8.56, N 1.46, S, 7.52%. Calculated: C 82.57, H 9.41, N 1.44, S, 6.58%. GPC: M_n = 4757 g/mol, M_w = 12 293 g/mol, D = 2.58. ^{1}H NMR (250 MHz, CD_2Cl_2): δ 7.90 (s, 2H), 7.82 (m, 2H), 7.59 (m, 6H), 3.10 (t, 2H) 2.1 (m, 8H), 0.9 (m, 70H). ^{13}C NMR (62.5 MHz, CD_2Cl_2): δ 157.08, 155.50, 152.64, 151.26, 149.12, 148.53, 143.19, 140.82, 138.85, 131.28, 130.08, 128.40, 125.76, 120.43, 114.83,40.93, 32.17, 32.06, 31.95, 30.32, 28.24, 24.24, 22.95, 14.18.

Result and Discussion

Monomer **M1** was synthesized in four steps (Scheme 1) from commercially available methyl 3-aminothiophene-2-carboxylate, which was converted to 3-aminothiophene according to the method of Huddleston and co-workers.[6] Subsequent reaction of 3-aminothiophene with heptanal under acidic conditions led to the formation of 4-hexylbithieno[3,2-*b*:2′3′-*e*]pyridine via transamination and dehydrogenation, as first described by Paulmier and co-workers.[7] Bromination of 4-hexylbithieno[3,2-*b*:2′3′-*e*]pyridine at the linear 2,6-positions proved problematic. Unfortunately, direct electrophilic bromination favored the nonlinear 3,7-positions; similar regiochemistry was reported for the bromination of thieno[3,2-*b*]pyridine.[17] As an alternative method, treatment of 4-hexylbithieno[3,2-*b*:2′3′-*e*]pyridine with *n*-butyllithium followed by an electrophilic bromine source (Br_2, NBS, CBr_4, or $BrCH_2CH_2Br$) was investigated as lithiation should favor the 2,6-positions. However, inseparable mixtures of mono-, di-, and tribrominated products were obtained in all cases as determined by GC-MS, presumably due to lithium−halogen rearrangements and competing electrophilic bromination. The solution adopted was to trap the dilithium salt as the bis(trimethyltin) derivative by reaction with trimethyltin chloride. Subsequent bromodestannylation by reaction with NBS in chloroform yielded monomer **M1** in excellent purity. The proposed regiochemistry was supported by NMR spectroscopy and is in good agreement with that reported for 2-bromothieno[3,2-*b*]pyridine.[17]

The alternating polymers **P1** and **P2** were synthesized (Scheme 2) by Suzuki coupling of **M1** with fluorene (**M2**) and indenofluorene (**M3**) bis(boronate)s in reasonable yields (67 and 75%, respectively). The number-

Scheme 2. Synthesis of Polymers P1 and P2

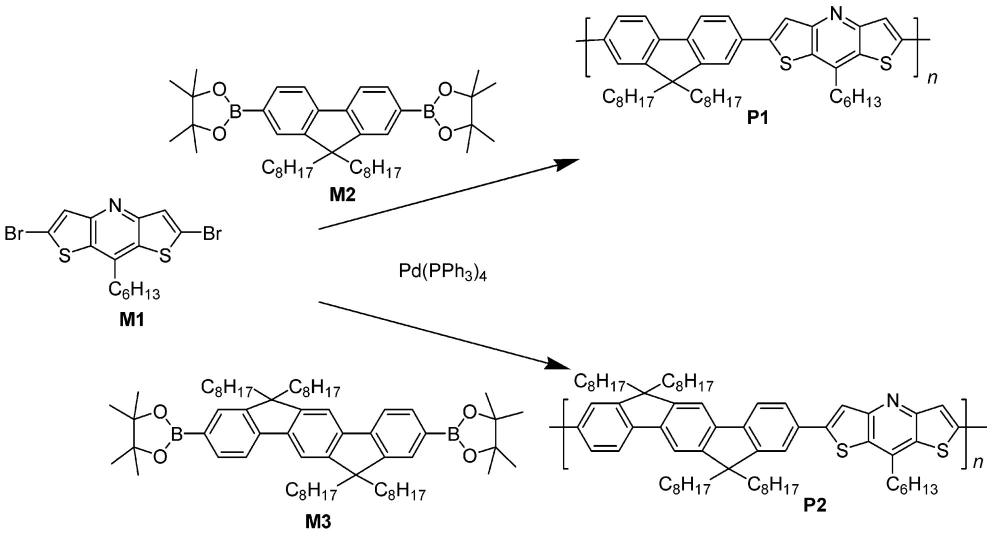

average molecular weights (M_n) of the polymers were determined by gel permeation chromatography (GPC) against polystyrene standards to be 11 000 for **P1** and 5000 for **P2** with polydispersities of 2.95 and 2.59, respectively. The molar masses of the polymers are much lower than for the corresponding fluorene and indenofluorene homopolymers. However, it is well-known that obtaining high molecular mass polymers by Suzuki polycondensation often requires careful optimization of the reaction conditions.[18] It is probable that such action in this case might significantly enhance the molar mass of the copolymers, but as both copolymers showed good film-forming properties despite their modest molecular weights we have not investigated this. The copolymers were readily soluble in common organic solvents such as chloroform, toluene, and tetrahydrofuran. **P2** showed better solubility and film-forming properties than **P1**. The chemical structures of the polymers were verified by NMR and elemental analysis. Both **P1** and **P2** showed high thermal stability by thermogravimetric analysis (TGA), with initial weight loss occurring at 443 and 447 °C, respectively.

The UV−vis absorption maxima of **P1** and **P2** in thin films appeared at 415 and 435 nm, respectively, which were only slight red-shifted from their values in solution, suggesting that there was little aggregation of the chromophores in the solid state (Figure 1). The red shift in the absorption of **P2** compared with **P1** is attributed to an increase of polymer chain planarity and effective conjugation length upon substitution of indenofluorene for fluorene.

Upon photoexcitation at 420 nm, both polymers exhibited blue-green emission with a peak in the blue at about 480 nm and another in the green (520−540 nm) (Figure 2). The positions of these peaks clearly show that there is extended conjugation in these materials, so that the lack of an bond alternated Kekulé form through the heterocyclic units alluded to in the Introduction obviously does not hinder the conjugation. The blue peak was dominant in the emission spectrum of **P1**, while the green emission was dominant for **P2**. The separation between the peaks was greater for **P1** (481 and 536 nm) than for **P2** (481 and 520 nm), and the relative intensity of the blue emission peak was higher for this polymer. Further investigations into the photophysics of these polymers in order to understand the reasons for the differences in the PL spectra are underway and will be reported separately.

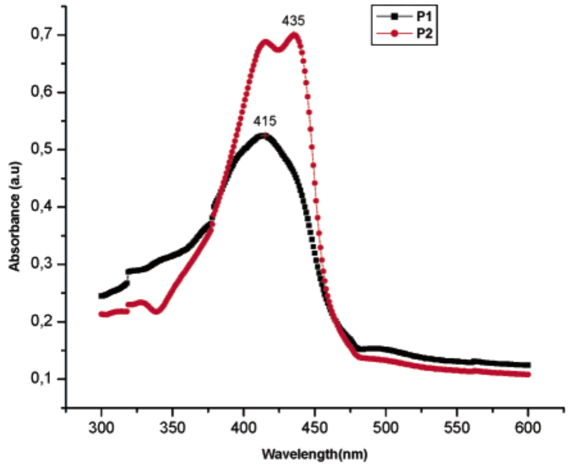

Figure 1. UV−vis absorption spectra of **P1** and **P2** as thin films.

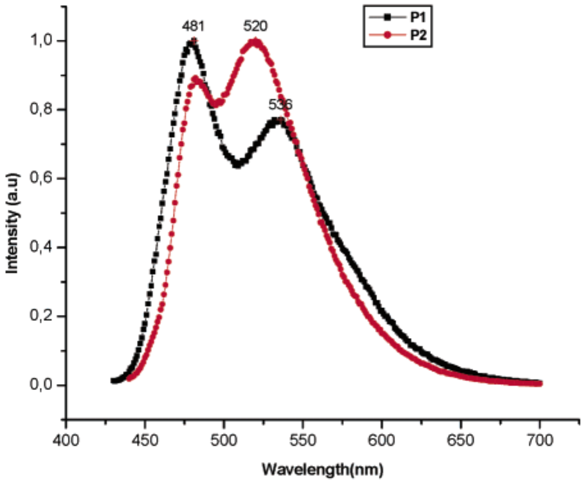

Figure 2. PL spectra of **P1** and **P2** films.

The electrochemical behavior of the polymers was investigated by cyclic voltammetry (CV) against Ag/Ag$^+$ by the method of Janietz.[19] As shown by the cyclic voltammograms in Figure 3, both polymers display n-doping and p-doping processes. As the energy level of Ag/AgCl is 4.4 eV below the vacuum level,[8] we deter-

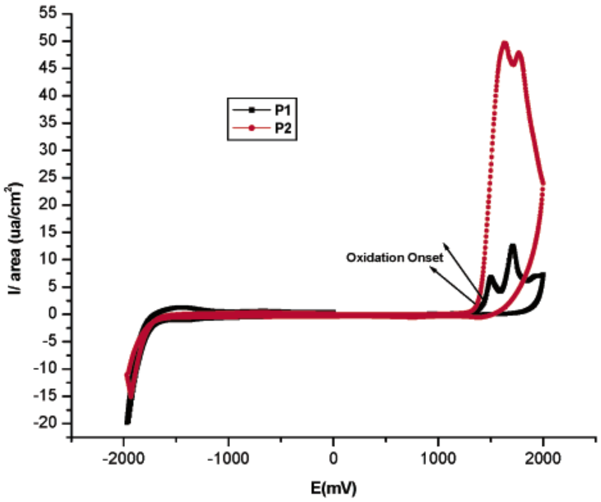

Figure 3. CV of **P1** and **P2**.

mined from the oxidation (1.32 V) and reduction (−1.61 V) onsets for **P1** the HOMO and LUMO energies to be respectively 5.76 and 2.79 eV. Similarly, from the corresponding potentials of 1.34 and −1.68 V for **P2** we calculated HOMO and LUMO energy levels of 5.74 and 2.72 eV, respectively. The resulting band gaps of 2.97 and 3.02 eV are slightly higher than the values of ca. 2.75 eV estimated from their absorption onsets. The HOMO energy levels for the copolymers are very similar to the value of 5.8 eV measured for polyfluorene homopolymers,[19] but the LUMO energy levels are significantly (>0.5 eV) lower than the values of 2.12[19] and 2.20 eV[13] previously reported for polyfluorenes, indicating that the bithienopyridine units have significantly improved the electron-accepting properties of the copolymers. Similar reduction and oxidation potentials have been observed in a statistical copolymer of fluorene and 2,5-pyridine (7:3),[20] suggesting that the redox properties of dithienopyridine are similar to those of pyridine.

To determine the effects of the bithienopyridine units on the packing of the polymer chains, we examined thin films of the polymers by tapping-mode atomic force microscopy. We have recently shown[10,21] that the microscopic morphology of thin films of conjugated polymers, as imaged with AFM, is a direct signature of the ability of the chains to pack into compact, regular π-stacks. Figure 4 (left) shows the microscopic morphology of a thin deposit of **P1** on mica. Unlike poly(dioctylfluorene), which forms fibrillar structures due to highly regular π-stacking,[21] **P1** are made up of aggregates of various sizes and shapes. This lack of fibrillar organization may partially reflect the relatively high polydispersity of **P1**, as large differences in segment lengths in polydisperse samples can act as defects preventing the formation of organized structures. However, we propose that the most important reason for the formation of nonorganized films is that the combination of the bithienopyridine and fluorene units alternating along the chains disrupts the chain linearity (compared to homo-polyfluorene), which probably reduces the $\pi-\pi$ intermolecular interactions and hence the stacking of the polymer chains. Under the same conditions, **P2** on mica (Figure 4, right) forms very thin platelets with a constant height of 1.3 nm, which is consistent with the thickness of a monolayer in which the planes of the conjugated segments are tilted relative to the substrate plane. This suggests that supramolecular order exists to a certain extent in this system. Chains with alternating bithienopyridine and indenofluorene are more likely to be linear and planar compared to **P1** chains, which is consistent with the red shift observed in the solid-state absorption spectra. Therefore, chain packing is expected to be more regular in **P2** than **P1**. However, unlike for the polyindenofluorene homopolymer,[10] no fibrillar morphology is observed, which is a clear sign that no long-range order exists in deposits of **P2**. This lack of fibrillar morphology means that exciton migration to defect sites is likely to be hindered compared with the homopolymers, which should reduce the amount of long wavelength emission from them. We have previously shown that there is a strong correlation between the degree of fibrillar morphology and the amount of long wavelength emission in the solid-state luminescence spectra of polyindenofluorenes.[10]

Electroluminescence Properties. To test the effect of the electron-accepting units on the EL properties of the copolymers, LEDs were constructed. Given the large offset between the HOMO energy levels of **P1** and **P2** and the work function of ITO (4.8−5.0 eV), a PEDOT:

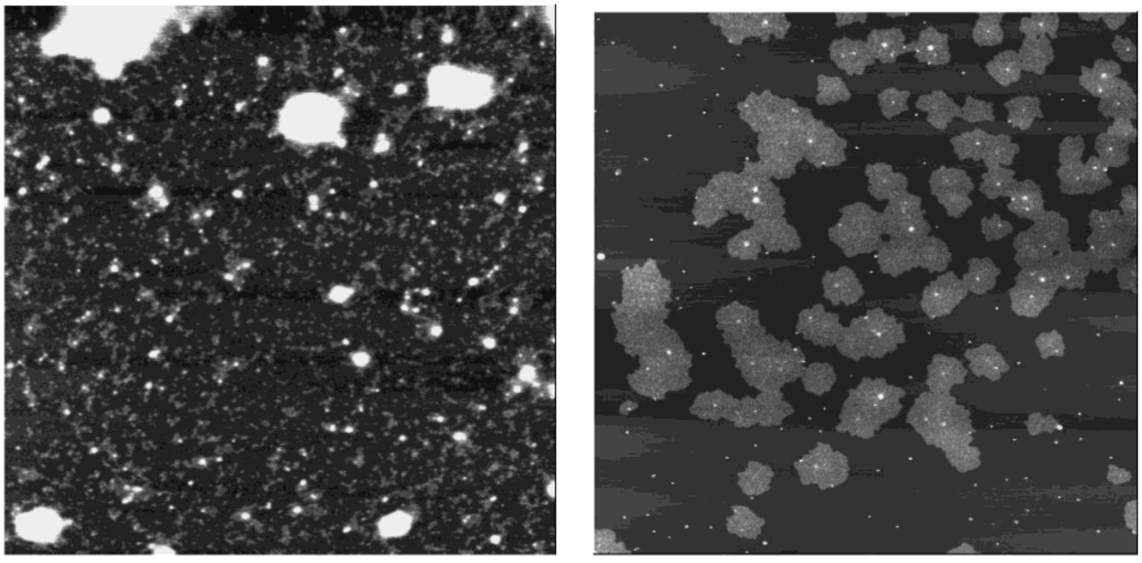

Figure 4. 4 × 4 μm^2 TM-AFM height images of thin deposits prepared from 0.05 mg/mL THF solutions on mica: left, **P1**; right, **P2**. The vertical gray scale is 5 nm for both images.

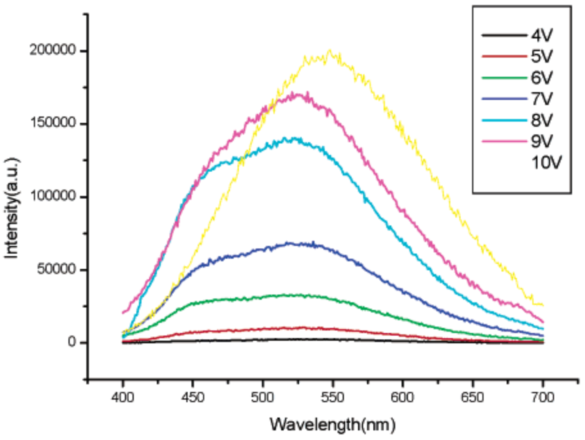

Figure 5. EL spectrum of ITO/PEDOT:PSS/**P1**/Al.

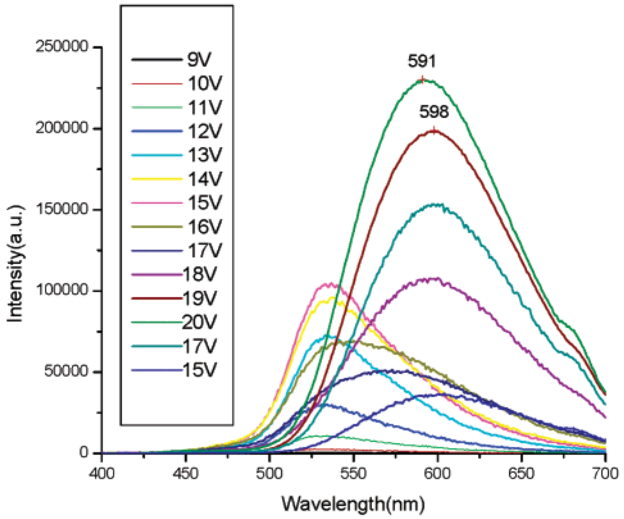

Figure 6. EL spectrum of ITO/PEDOT:PSS/**P2**/Al.

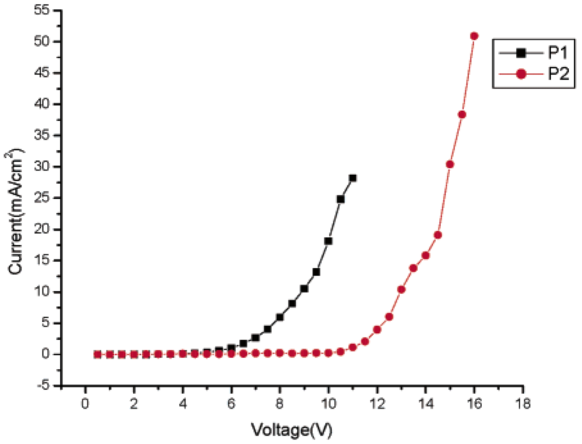

Figure 7. *I*−*V* characteristics for ITO/PEDOT:PSS/**P1**/Al (black) and ITO/PEDOT:PSS/**P2**/Al (red).

PSS hole-transporting layer (5.3−5.4 eV) was used. Normally with fluorene or indenofluorene-based polymers calcium cathodes (work function 2.9 eV) are used to get efficient electron injection, but in order to test whether the electron-accepting bithienopyridine units had significantly improved the electron affinity of the copolymers we used aluminum cathodes (work function 4.2 eV). As these are only preliminary studies, no attempt was made to optimize the device fabrication or performance.

The electroluminescence (EL) spectra for the devices are shown for various applied voltages. The EL behavior of the two copolymers was quite different with increasing voltage. In the case of **P1** (Figure 5) the EL spectrum initially consisted of a single broad featureless band between 450 and 600 nm, comprising both the blue-green band at 480 nm and the green band at 536 nm seen in the PL spectrum, with some broadening of the emission bands. There was a slight increase in the relative intensity in the green emission band with increasing voltage from 6 to 9 V, and at 10 V there was a notable red shift in the emission, consistent with the emission now coming only from the green band. The EL spectrum remained constant at higher voltage, and the changes were reversible, indicating that this change was not due to any irreversible chemical or morphological change. One possible explanation is that there is some doping of the polymer at the interfaces with the PEDOT or the cathode which affects the emission properties and that the change in color is due to a shift in the recombination zone toward these doped regions. Other possible causes are that the relative formation of excitons on the copolymer units may be field-dependent or that we are seeing field-dependent formation of exciplexes or excimers. We have observed similar effects in copolymers of fluorene and pyridine, and further studies are underway to elucidate the mechanisms of the observed color changes in those materials.[20]

By contrast, the EL spectrum of **P2** (Figure 6) showed an irreversible red shift above 15 V, with the EL maximum moving from 534 to 591 nm. Such an irreversible change must reflect a chemical or morphological change in the material.

A similar irreversible red shift has been seen at lower voltages for tetraalkylindenofluorene homopolymers, even those which show no long-range order in their thin-film morphology.[10] As evidence from delayed PL studies[22] suggests the long wavelength emission from poly(tetraoctylindenofluorene), like that from polyfluorenes, is dominated by emission from ketone defects, we propose that the change is due to an electrochemically promoted oxidation of the indenofluorene units in **P2**. That the change occurs at higher potentials than for the indenofluorene homopolymers suggests that the electron-accepting units are to some extent protecting the indenofluorene units. The nonobservation of a similar oxidation in **P1** may be due to the fact that fluorenone emission occurs at about 530 nm, and so any emission from defects would be masked by the existing band at 536 nm.

Figure 7 shows the current density as a function of applied voltage for the devices. From these it can be seen that **P1** has a significantly lower onset voltage (5 vs 11 V), but this may reflect differences in the device fabrication, as it has been shown that minor variations in cathode deposition rates can significantly affect device performance.[23] By contrast, the efficiency of the device using **P2** (0.74 cd/A) was an order of magnitude higher than for that using **P1**, for which the most obvious explanation is that the better chain packing in **P2** results in higher charge carrier mobility. However, as no attempt has been made to optimize these devices, it is premature to derive any firm conclusions from these results. Further, more detailed investigations into LEDs containing the copolymers are underway in order to elucidate the mechanisms behind the color changes, and other behavior and will be reported separately.

These results clearly show that bithieno[3,2-*b*:2′,3′-*e*]pyridine is a good electron-accepting unit, whose incorporation into conjugated polymers may significantly improve their performance in LEDs by improving electron injection and transport. These results suggest that it can also provide some protection against oxidative degradation during device operation.

Conclusions

A novel electron-accepting 2,6-dibromobithieno[3,2-*b*:2′,3′-*e*]pyridine has been prepared and copolymerized with fluorene and indenofluorene to make blue-green emitting copolymers. Electrochemical data prove that the heterocyclic units significantly improve the electron affinity of the copolymers. AFM analysis of the film morphologies shows no long-range order, suggesting that the heterocyclic moieties disrupt the chain packing especially in the fluorene copolymer. LEDs with high work-function aluminum cathodes using the copolymers produce blue-green emission with low turn-on voltages, confirming their improved electron-accepting properties. Whereas the fluorene copolymer shows relatively stable emission at high voltages, the indenofluorene-based copolymer shows an irreversible red shift in emission above 15 V, which is attributed to oxidation of the polymer. Both copolymers show more stable emission at lower voltages than the corresponding homopolymers, suggesting that the electron-accepting moieties provide some protection against electrochemical oxidation.

Acknowledgment. This work was supported by the Bundesministerium für Bildung und Forschung through Project PODOS. The collaboration between Mons and Mainz is conducted within the framework of the Inter-University Attraction Pole Program (PAI V/3) of the Belgian Federal Government and the European Science Foundation “Structuring, Manipulation, Analysis and Reactive Transformation of Nanostructures (SMARTON)” program. Research in Mons is supported by the European Commission and the Government of the Région Wallonne (Phasing Out−Hainaut) and the Belgian National Fund for Scientific Research FNRS/FRFC. R.L. is Directeur de Recherches du F.N.R.S. M.S. acknowledges the F.R.I.A. for a doctoral scholarship. We thank Dr. Emil List (Technical University of Graz) for some helpful suggestions concerning the interpretation of the EL results.

References and Notes

(1) Dimitrakopoulos, C. D.; Malenfant, P. R. L. *Adv. Mater.*. **2002**, *14*, 99−117.
(2) Brabec, C. J.; Sariciftci , N. S.; Hummelen, J. C. *Adv. Funct. Mater.* **2001**, *11*, 15−26.
(3) Kraft, A.; Grimsdale, A. C.; Holmes, A. B. *Angew. Chem., Int. Ed.* **1998**, *37*, 402−428.
(4) Mitschke, U.; Bäuerle, P. *J. Mater. Chem.* **2000**, *10*, 1471−1507.
(5) Lu, H.-F.; Chan, H. S. D. O.; Ng, S.-C. *Macromolecules* **2003**, *36*, 1543−1552.
(6) Barker, J. M.; Huddleston, P. R.; Wood, M. L. *Synth. Commun.*. **1995**, *25*, 3729−3734.
(7) Berkaoui, M.; Outurquin, F.; Paulmier, C. *J. Heterocycl. Chem.* **1996**, *33*, 9−16.
(8) (a) Neher, D. *Macromol. Rapid Commun.* **2001**, *22*, 1365−1385. (b) Leclerc, M. *Polymer* **2001**, *39*, 2867.
(9) Setayesh, S.; Marsitzky, D.; Müllen, K. *Macromolecules* **2000**, *33*, 2016−2020.
(10) Grimsdale, A. C.; Leclère, Ph.; Lazzaroni, R.; MacKenzie, J. D.; Murphy, C.; Setayesh, S.; Silva, C.; Friend, R. H.; Müllen, K. *Adv. Funct. Mater.* **2002**, *12*, 729−733.
(11) Scherf, U.; List, E. J. W. *Adv. Mater.* **2002**, *14*, 477−487.
(12) Setayesh, S.; Grimsdale, A. C.; Weil, T.; Enklemann, V.; Müllen, K.; Meghdadi, F.; List, E. J. W.; Leising, G. *J. Am. Chem. Soc.*. **2001**, *123*, 946−953.
(13) Ego, Ch.; Grimsdale, A. C.; Uckert, F.; Yu, G.; Srdanov, G.; Müllen, K. *Adv. Mater.* **2002**, *14*, 809−812.
(14) Pogantsch, A.; Wenzl, F. P.; List, E. J. W.; Leising, G.; Grimsdale, A. C.; Müllen, K. *Adv. Mater.* **2002**, *14*, 1061−1064.
(15) Jacob, J.; Zhang, J.; Grimsdale, A. C.; Müllen, K.; Gaal, M.; List, E. J. W. *Macromolecules* **2003**, *36*, 8240−8245.
(16) Sainova, D.; Miteva, T.; Nothofer, H.-G.; Scherf, U.; Glowacki, I.; Ulanski, J.; Fujikawa, H.; Neher, D. *Appl. Phys. Lett.*. **2000**, *76*, 1810−1812.
(17) Klemm, L. H.; Louris, J. N. *J. Heterocycl. Chem.* **1984**, *21*, 785−789.
(18) Schlüter, A. D. *J. Polym. Sci., Part A: Polym. Chem.* **2001**, *39*, 1533−1556.
(19) Janietz, S.; Bradley, D. D. C.; Grell, M.; Giebeler, C.; Inbasekaran, M.; Woo, E. P. *Appl. Phys. Lett.* **1998**, *73*, 2453−2455.
(20) Sonar, P.; Zhang, J.; Grimsdale, A. C.; Müllen, K. Unpublished results.
(21) Leclère, Ph.; Hennebicq, E.; Calderone, A.; Brocorens, P.; Grimsdale, A. C.; Müllen, K.; Brédas, J. L.; Lazzaroni, R. *Prog. Polym. Sci.* **2003**, *28*, 55−81.
(22) Keivanidis, P. E.; Im, C.; Lupton, J M.; Jacob, J.; Grimsdale, A. C.; Müllen, K. Unpublished results.
(23) Koch, N.; Pogantsch, A.; List, E. J. W.; Leising, G.; Blyth, R. I. R.; Ramsey, M. G.; Netzer, F. P. *Appl. Phys. Lett.* **1999**, *74*, 2909−2911.

MA035329U